Polymer Journal (2024) 56:473–480
https://doi.org/10.1038/s41428-024-00889-7

ORIGINAL ARTICLE

Fluorophore-glucan conjugate for oligosaccharide sensing in aqueous media

Hiroki Kurohara[1] · Yumiko Hori[2] · Munenori Numata[3] · Gaku Fukuhara[2]

Received: 13 December 2023 / Revised: 7 January 2024 / Accepted: 8 January 2024 / Published online: 7 February 2024

Abstract

The ability to sense saccharides in aqueous media using conventional supramolecular approaches was a turning point in modern chemistry. Herein, we performed oligosaccharide sensing using fluorophore-modified branched glucans. Through the newly developed glucan-based chemosensor, acarbose sensing was achieved in a selectively and sensitive manner. The optical properties and morphological changes in the chemosensor were investigated, revealing that the globule-to-coaggregation process plays a key role in oligosaccharide sensing.

Introduction

Saccharide (sugar) recognition using synthetic receptors or chemosensors in aqueous media has been extensively investigated because the process is very important for a range of biomedical applications [1–13]. Nevertheless, further practical applications in this field are currently hampered by numerous drawbacks. Methods to monitor biologically important oligosaccharides as tumor markers in real-time are highly desirable [14, 15]. Unfortunately, methods that sense oligosaccharides in a selective and sensitive manner are currently inefficient because the target oligosaccharides in the blood exhibit conformational complexity, extensive solvation (hydration), and extremely low concentration [6, 12, 16].

To date, two strategies have been successfully used for saccharide sensing. Boronic acid-incorporated chemosensors capture mono- and disaccharides through dynamic boronate formation [17–25]. Second, water-soluble supramolecular cages, or artificial lectins, are functional examples in which oligosaccharides are placed in the cavity through hydrophobic effects and multiple CH-π interactions [26–38]. However, neither method performs satisfactorily in real-life applications. The inherent problem of the supramolecular approach is its lock-and-key or "rigid" mechanism; the cage cavity must be expanded in a step-by-step manner to fit the target oligosaccharide closely, which is unrealistic. An attractive alternative for creating "smarter" chemosensors with oligosaccharide-sensing control is an induced-fit approach, which is flexible and dynamic. Nature adopts induced-fit mechanisms for sugar chain recognition. For example, lectins utilize the cooperativity of highly ordered hydrogen-bonding networks and CH-π interactions [39], which can serve as a blueprint for designing smart dynamic chemosensor systems.

In 2010, we discovered that curdlan (Cur) functions as a selective and sensitive oligosaccharide chemosensor through interactions within the dynamic hydrogen-bonding networks of the Cur polymer backbone [40]. Cur (Fig. 1a, top) is the simplest glucan, as it possesses a linear backbone and consists of β-(1,3)-linked D-glucose units. The most intriguing characteristic of native glucans is their reversible denaturing/renaturing behavior, which leads to the formation of random coils in DMSO and triplexes in aqueous solutions [41–43]. Therefore, we focused on the reversibility of Cur, hypothesizing that oligosaccharides become

Supplementary information The online version contains supplementary material available at https://doi.org/10.1038/s41428-024-00889-7.

✉ Gaku Fukuhara
gaku@chem.titech.ac.jp

[1] Department of Applied Chemistry, Osaka University, 2-1 Yamada-oka, Suita 565-0871, Japan

[2] Department of Chemistry, Tokyo Institute of Technology, 2-12-1 Ookayama, Meguro-ku, Tokyo 152-8551, Japan

[3] Department of Biomolecular Chemistry, Graduate School of Life and Environmental Sciences, Kyoto Prefectural University, Shimogamo, Sakyo-ku, Kyoto 606-8522, Japan

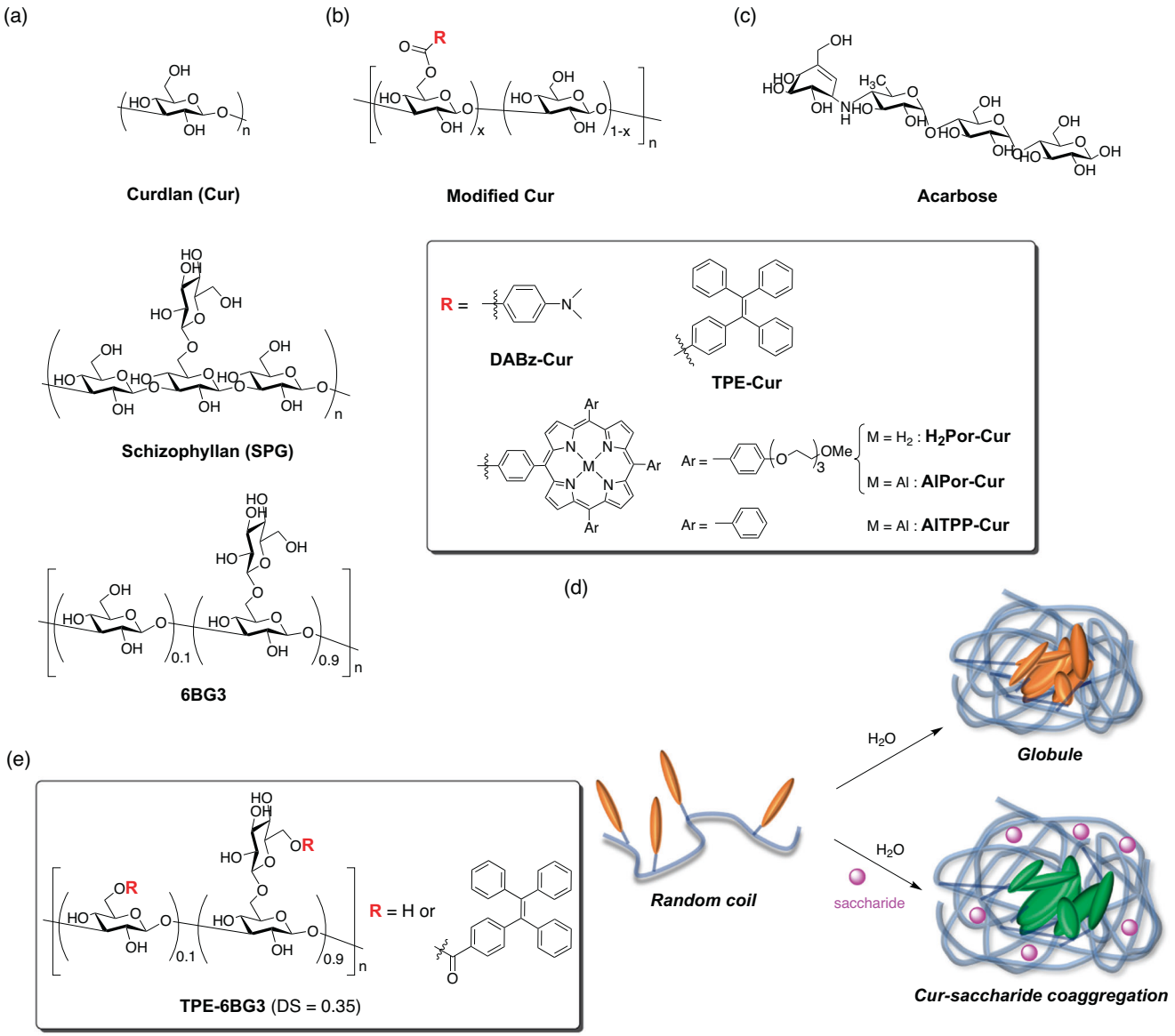

Fig. 1 Chemical structures of (**a**) glucans, curdlan (Cur), schizophyllan (SPG), and highly branched glucan (**6BG3**); (**b**) modified Cur; (**c**) acarbose; and **d** Schematic representation of the reversible dynamic morphological changes in modified Cur in aqueous media: random coil-to-globule (*top*) and -cur-saccharide coaggregation (*bottom*) processes. **e TPE-6BG3**

trapped after splicing into Cur strings during the renaturing process. As a first prototype shown in Fig. 1b, the modified Cur glucan bearing 4-dimethylaminobenzoate was developed as a reporter to sense the tetrasaccharide acarbose (Fig. 1c) in aqueous media in a selective and sensitive manner [40]. Although acarbose is used worldwide to treat type 2 diabetes and obesity, the medication causes unwanted side effects; thus, methods to monitor acarbose concentrations in blood, which is an aqueous solution, in real-time are highly desirable [44]. During our acarbose-sensing investigation using modified Curs, we established that morphological changes in the modified Cur induced by switching the solvent from DMSO to an aqueous medium play a significant role in sensing [45]. Namely, as shown in Fig. 1d, the random-coiled string of the modified Cur in DMSO changes to a globule in aqueous media, which selectively captures acarbose in dynamic and flexible strings, generating Cur-saccharide coaggregation. Based on the sensing mechanism, the limits of detection (LODs) were significantly improved from 10 mM for **DABz-Cur** [40] to 5 mM for **H_2Por-Cur** [45], 200 μM for **AlPor-Cur** [45], 100 μM for **AlTPP-Cur** [46], and 5 μM for **TPE-Cur** [47] by varying the reporter (see structures in Fig. 1b). Previous studies have noted the appreciable efficacy of the fluorescent reporter TPE compared to the circular dichroism chromophores DABz and Por. Therefore, exploring novel dynamic polymer backbones that can trap oligosaccharides is very important.

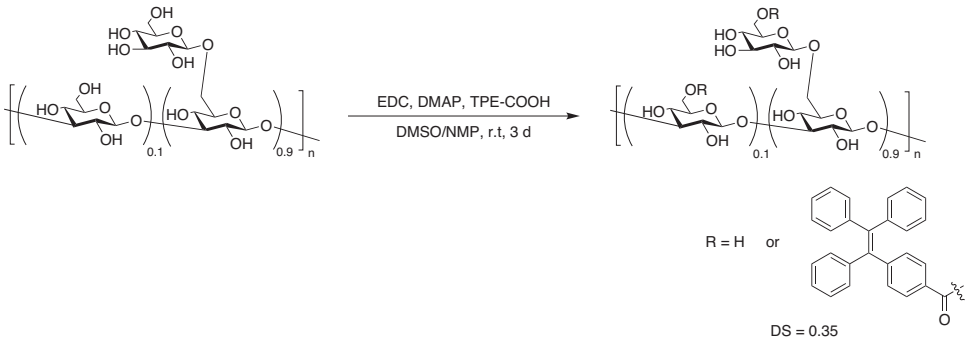

Fig. 2 Synthetic scheme of **TPE-6BG3**

In this study, to expand the range of glucans and explore this new possibility, we focused on the highly branched glucan **6BG3** (Fig. 1a, *bottom*), which is a 1,6-glucose-branched β-1,3-glucan, rather than other branched glucans, such as schizophyllan (SPG) (Fig. 1a, *center*). Recently, we established that **6BG3** also possesses denaturing/renaturing characteristics based on random coil-to-globule conversion, as observed for Cur [48]. These findings suggest that **6BG3** can function as a dynamic, flexible, and induced-fit type of oligosaccharide chemosensor. This prompted us to investigate the type of oligosaccharide recognized by **6BG3** in aqueous media, the extent of recognition, and the underlying mechanism. Herein, we report the oligosaccharide-sensing behavior of the fluorophore-probed **6BG3** (Fig. 1e) in aqueous media. According to previous reports on Cur chemosensors, the TPE fluorophore is suitable for the present purpose. This comparative study of **6BG3** vs. Cur provides new insights into the factors that govern oligosaccharide-sensing outcomes when using glucans.

Experimental procedure

Materials

Spectroscopic-grade DMSO, Milli-Q H_2O, and commercially available nonaminosaccharides were used as received. **6BG3** (degree of glucose branching = 90%) was supplied by DS Wellfoods Co., Ltd., and was dried at 60 °C under high vacuum prior to use. The number-average weight (M_n) and polydispersity index (PDI) of **6BG3** were previously determined to be 3300 and 3.9, respectively [48]. Glucosamine and validamycin A, available in acidic form, were neutralized by adding an appropriate amount of aqueous KOH to DMSO containing **TPE-6BG3**. All polymer concentrations are expressed in chromophore units unless noted otherwise.

AFM measurements

A 1:9 (v/v) DMSO-H_2O solution of native **6BG3** or **TPE-6BG3** was dropped onto the mica surface, predried under N_2 gas flow, and dried under high vacuum prior to AFM observation.

Saccharide-sensing procedure

Sample solutions of **TPE-6BG3** in 1:9 (v/v) DMSO-H_2O were prepared; a portion of the stock DMSO solution containing **TPE-6BG3** and the target saccharide was diluted with H_2O. The resulting mixture was further stirred for 10 min and subsequently subjected to fluorescence spectroscopy.

Synthesis of TPE-6BG3

The synthetic scheme was shown in Fig. 2. **6BG3** (120 mg, 0.39 mmol in glucose units) was added to dry DMSO (2 mL) in a three-necked flask. The solution was heated at 70 °C for 1 h, followed by the addition of *N*-methyl-2-pyrrolidinone (NMP) (18 mL). The resulting highly viscous solution was stirred at 90 °C overnight. After cooling to room temperature, TPE-COOH (84 mg, 0.22 mmol) was dissolved in the solution. Subsequently, 1-ethyl-3-(3-dimethylaminopropyl)carbodiimide hydrochloride (EDC) (425 mg, 2.22 mmol) and *N*,*N*-dimethyl-4-aminopyridine (DMAP) (220 mg, 2.22 mmol) were added to the DMSO/NMP solution, and the mixture was stirred for 3 days. To promote the reaction, EDC (426 mg, 2.22 mmol) and DMAP (220 mg, 2.22 mmol) were added every 24 h. After three days, the reaction mixture was slowly poured into methanol (200 mL), and a white precipitate was generated. This precipitate was collected, washed with methanol (3 × 50 mL), and dried under high vacuum to afford **TPE-6BG3** in 64% yield (135 mg, 0.25 mmol in monomer unit) as a white solid. ^{1}H NMR (400 MHz, DMSO-d_6, 25 °C) δ_H 7.71 (H_7), 7.12 (H_8), 6.97 (H_8), 5.22–2.98 (sugar protons); ^{13}C NMR (150 MHz, DMSO-d_6, 25 °C) δ_C 143.1 (C_{Ar}), 140.1 (C_{Ar}), 131.1–127.4 (C_{Ar}), 103.6 (C1), 86.6 (C3), 77.1, 76.8, 75.1, 74.2, 73.0, 70.5, 68.9, 61.4 (C6); IR ν 3426, 2895, 2360, 2135, 1716, 1645, 1445, 1026, 750, 700 cm^{-1}. The degree of substitution (DS) for **TPE-6BG3** was determined by comparing the molar extinction coefficient

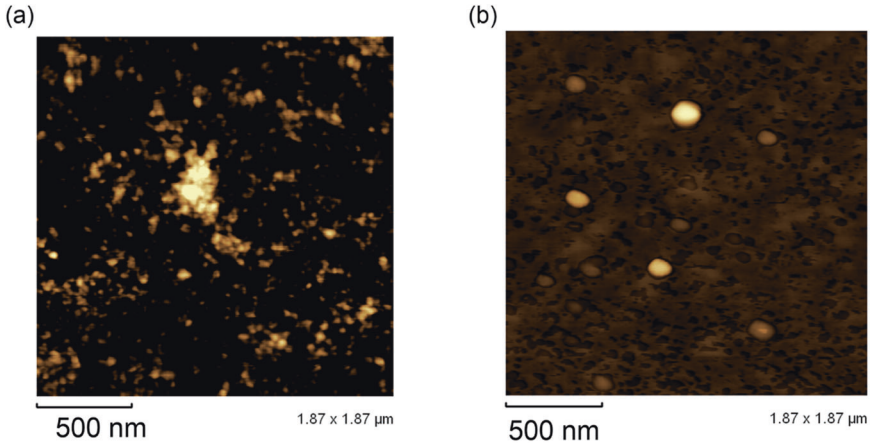

Fig. 3 AFM images of (**a**) native **6BG3** (data from ref. 48) and (**b**) **TPE-6BG3** prepared from 1:9 (v/v) DMSO-H_2O solutions drop-casted on mica surfaces

(ε) of authentic anionic TPE-COOH and the TPE-COOH liberated from **TPE-6BG3** upon hydrolysis. A 5:95 (v/v) aqueous KOH-DMSO solution of **TPE-6BG3** (0.094 g/L) was stirred for hydrolysis and monitored via UV/vis spectroscopy. After hydrolysis (21 h) was completed, the absorbance at 310 nm was 0.57579. Thus, the concentration of liberated TPE-COO^- from **TPE-6BG3** was estimated to be 4.89×10^{-5} M based on the ε = 11772 of TPE-COO^-. When the DS of **TPE-6BG3** was 1, the concentration of liberated TPE-COO^- was calculated to be 1.41×10^{-4} M (= 0.094/666.51). Thus, the DS can be estimated as 0.35 ($= 4.89 \times 10^{-5}/1.41 \times 10^{-4}$). **TPE-6BG3**, with a DS of 0.35, was soluble in DMSO and in 1:9 (v/v) DMSO-H_2O.

Results and discussion

For this purpose, the best-performing TPE chromophore for aggregation-induced emission (AIE) [49] was attached to the **6BG3** backbone as a reporter to afford **TPE-6BG3** with a degree of substitution (DS) of 0.35 (Fig. 1e) (see NMR spectra in the Supplementary Information (SI)). First, we investigated the morphological changes in **TPE-6BG3** using atomic force microscopy (AFM). An aqueous solution (1:9 (v/v) DMSO-H_2O) of native (nonmodified) **6BG3** was drop-cast onto mica and then completely dried. The AFM image of **6BG3** shown in Fig. 3a reveals a dispersed/diverse structure, as previously reported [48], indicating that a renatured macromolecular structure similar to that of other glucans was formed [45–47]. In contrast, the AFM image of mica obtained from the aqueous solution of **TPE-6BG3** exhibited a dotted, globular morphology in the renatured state (Fig. 3b). The height and width of the globules were estimated to be 8.6 ± 5.9 nm ($n = 13$) and 125 ± 32 nm ($n = 12$), respectively (Fig. S2 in the SI). These morphological changes (random coil-to-globule conversions induced by modifications of the chromophore on the glucan backbone) are very likely to be common in glucan chemistry.

Next, the photophysical properties of **TPE-6BG3** were analyzed in solution to investigate the effects of these morphological changes on the fluorescence behavior. As shown in Fig. 4a (black line, *inset*), the DMSO solution of **TPE-6BG3** displayed negligible fluorescence across the wavelength range, indicating that the phenyl rings in the TPE luminogen moved freely on the randomly coiled **6BG3** backbone. Interestingly, the fluorescence spectrum for the aqueous DMSO solution of **TPE-6BG3** (Fig. 4a, red line) was intense due to the aggregation of the TPE luminogen based on its AIE character, which is consistent with globule formation in aqueous media; the appended TPE chromophores aggregated in the globules formed by the dynamic **6BG3** backbone, affecting high emission. The fluorescence quantum yield (Φ_F) of **TPE-6BG3** in aqueous DMSO was sufficient for detection (0.30), in contrast to its undetectable Φ_F in DMSO. Direct evidence of globule formation was obtained using dynamic light scattering (DLS) measurements. As shown in Fig. 4b (black line), the DLS data obtained in aqueous DMSO indicated the presence of monodisperse particles with a hydrodynamic diameter (d_h) of 43 nm. To elucidate the origin of the excited species, the fluorescence lifetimes of **TPE-6BG3** were obtained. The decay profiles obtained in aqueous media were not subjected to regular deconvolution fitting, as the number of excited species cannot be determined due to the globular ensemble of the TPE fluorophores. Therefore, in this situation, the stretched exponential function (Kohlrausch decay) model (Eq. 1) appears to be more suitable for polymeric systems [50, 51]:

$$I(t) = I_0 \exp[(-(t/\tau)]^{\beta} \quad (1)$$

where I_0 and $I(t)$ express the photon counts at the initial and arbitrary times, respectively, τ is the average lifetime, and β is the dispersion factor ($0 < \beta < 1$). As shown in Fig. 4c (*left*), the decay profiles of **TPE-6BG3** in aqueous DMSO were fitted using Eq. 1 to obtain τ and β as 2.7 ns and 0.86,

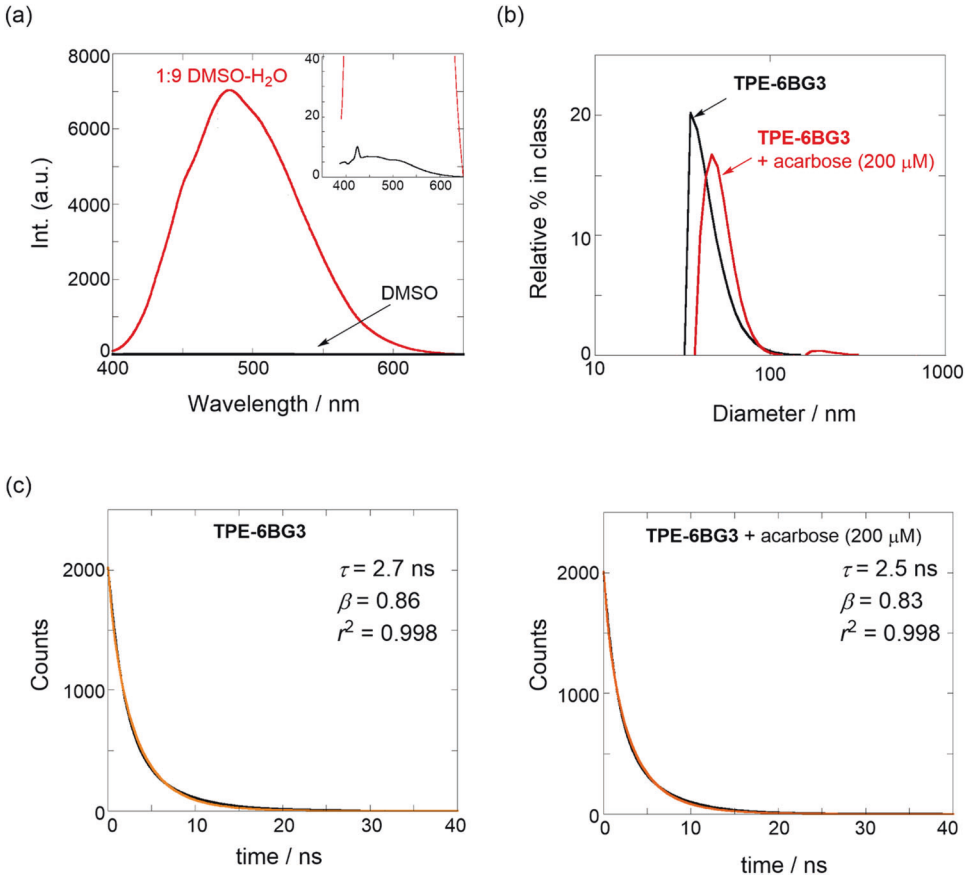

Fig. 4 **a** Fluorescence spectra (λ_{ex} 378 nm) of **TPE-6BG3** (36 μM) in DMSO (black) and in 1:9 (v/v) DMSO-H_2O at 25 °C. **b** DLS profiles of 1:9 (v/v) DMSO-H_2O solutions of **TPE-6BG3** (9 μM) without (black) and with acarbose (200 μM, red). **c** Fluorescence lifetime decays (black) of 1:9 (v/v) DMSO-H_2O solutions of **TPE-6BG3** (9 μM) without (left) and with acarbose (200 μM, right). The orange lines show the fitting results

respectively. Next, the changes in optical and particle characteristics upon complexation with oligosaccharides were investigated.

To explore the selectivity of the dynamic globulization of **TPE-6BG3**, we tested its response to various saccharides, ranging from mono- to hexasaccharides (see structures in Fig. 5a); the globule was retained at least during the spectroscopic examinations. As shown in Fig. 5b, the fluorescence intensities of all the examined saccharides decreased for **TPE-6BG3** upon complexation with saccharides (see Figs. S3–6 in the SI for detailed data). Notably, acarbose and its analog, validamycin A, induced markedly enhanced fluorescence, indicating that robust interactions occurred between the dynamic **6BG3** backbone and acarbose. Interestingly, the data in Fig. 5c (red regression line) show that the fluorescence changes were strongly correlated with the length of the saccharide skeleton. Therefore, the extensive hydrogen bonding network in the **6BG3** backbone plays a significant role in the sensing behavior. Among the saccharides tested, acarbose and validamycin A possess a valienamine structure (red moiety in Fig. 5a) and may interact strongly with the dynamic **6BG3** globule. Thus, the responses to glucosamine, which bears a hydrogen-bond donor amino group, and hydrophobic fucose, which has a methyl group, were compared to those to the corresponding monosaccharide, glucose. Based on the results, the former compounds induced more pronounced changes in fluorescence intensity. This result further supports the hypothesis that the high selectivity of the **6BG3** globule for acarbose (valienamine + maltotriose) led to the difference. We found that **6BG3**, a glucan, also exhibited high selectivity toward the acarbose skeleton. This discovery of acarbose sensitivity could apply to general glucans, such as SPG and other branched glucans. Titration experiments were also conducted to determine the sensitivity for acarbose using the **TPE-6BG3** chemosensor. As shown in Fig. 5d, the AIE intensities gradually decreased upon complexation of acarbose with **TPE-6BG3**, indicating that the dynamic globules expanded (*vide infra*). In Fig. 5e, the slope of the linear decrease, which was obtained from Δ_{int} versus the concentration of acarbose (μM), was calculated to be –3.51 and was used as the sensitivity parameter, $\Delta_{int} = -y$ [acarbose (μM)]; the value obtained is smaller than that (–5.94) of **TPE-Cur** (DS = 13%) [47]. Furthermore, the LOD for acarbose obtained using **TPE-6BG3** was determined to be 10 μM (see Fig. S7 and the present LOD definition in SI); the LOD obtained using **TPE-Cur** was 5 μM, as described above. The differences between **6BG3** and **Cur** are most likely responsible for the looser renaturing behavior [48] based on the highly branched glucose on the glucan backbone.

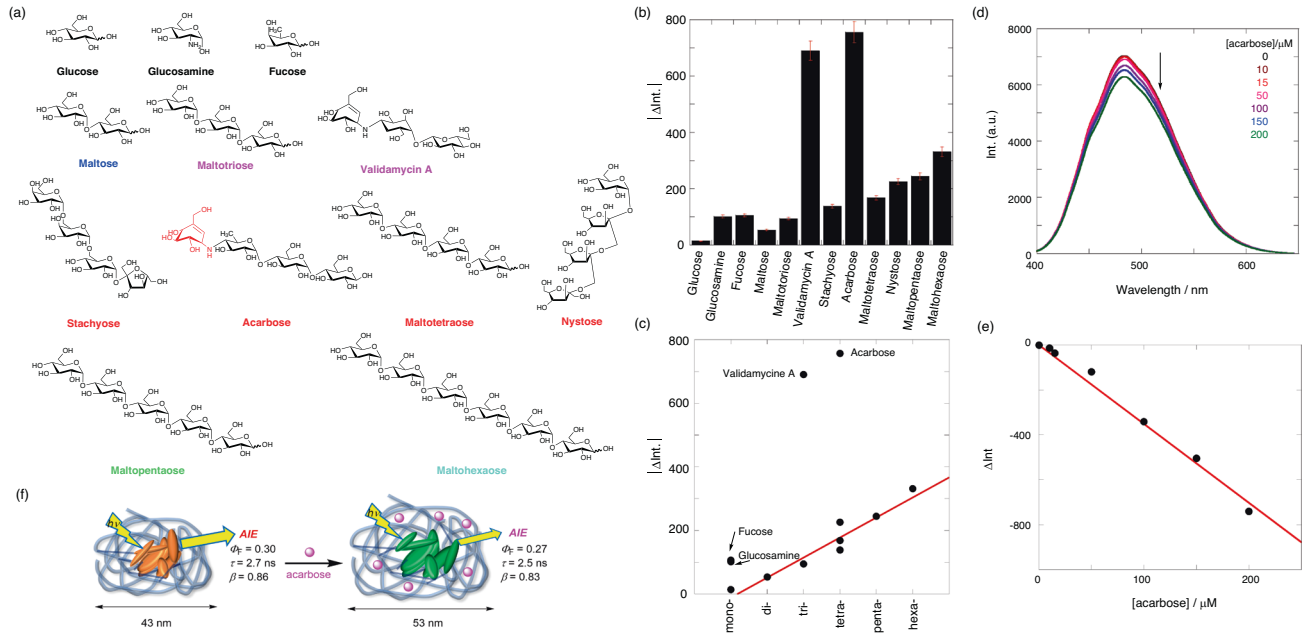

Fig. 5 **a** Chemical structures of the tested saccharides (mono- to hexasaccharides). **b** ΔInt. (484 nm) of **TPE-6BG3** (36 μM) induced upon complexation of various saccharides (200 μM); ΔInt. represents the delta fluorescence intensity. **c** ΔInt. data plotted as a function of saccharide length. **d** Fluorescence spectra (λ_{ex} 378 nm) of **TPE-6BG3** (36 μM) in the absence (black) and presence (10, 15, 50, 100, 150, and 200 μM, colored lines) of acarbose in 1:9 (v/v) DMSO-H_2O at 25 °C; the excitation wavelengths applied were those at which comparable absorbances were obtained. **e** ΔInt. data were plotted as a function of the acarbose concentration; ΔInt. = –3.51 [acarbose (μM)]. **f** Schematic illustration of the changes in globule expansion-based AIE

To obtain mechanistic knowledge on the selective sensing of acarbose by **TPE-6BG3**, the abovementioned analyses were performed with acarbose. DLS analysis revealed a d_h of 53 nm (Fig. 4b, red line). The expanded globule structure resulted from the formation of **6BG3**-acarbose coaggregates, as illustrated in Fig. 5f. This finding is further supported by the gradual decrease in the AIE intensities upon the addition of acarbose, with a decreased Φ_F of 0.27. The decrease in fluorescence intensity upon the addition of acarbose can be explained by the restricted rotation of the phenyl rings in the TPE luminogen, which relaxed due to the expansion of the dynamic globule. Furthermore, the decay profile in the presence of acarbose was subjected to Eq. (1), which yielded τ and β values of 2.5 ns and 0.83, respectively. The shorter τ and high degree of β strongly indicate that the degree of freedom increased for the appended TPE chromophore, reinforcing the expansion of flexible and dynamic globular coaggregation.

Conclusions

In conclusion, we developed a glucan-based dynamic, induced-fit oligosaccharide chemosensor. The highly branched glucan **6BG3** traps acarbose, a clinical drug, in aqueous media. Acarbose sensing was achieved in a selective and sensitive manner via globule-to-glucan-saccharide coaggregation conversion. This sensing behavior may be general for all glucans. Therefore, the results obtained herein can serve as a guideline for the construction of new smart chemosensors based on a dynamic induced-fit approach, which may enable the sensing of complicated oligosaccharides and sugar chains, which are challenging to recognize using conventional lock-and-key-type chemosensors.

Acknowledgements GF acknowledges the generous support provided by Grants-in-Aid (Nos. 19H02746 and 23H04020) from the Japan Society for the Promotion of Science (JSPS). We are grateful to Prof. Yoshihisa Inoue at Osaka University for fruitful discussions.

Compliance with ethical standards

Conflict of interest The authors declare no competing interests.

References

1. James TD, Sandanayake KRAS, Shinkai S. Saccharide sensing with molecular receptors based on boronic acid. Angew Chem Int Ed Engl. 1996;35:1910–22.
2. Davis AP, Wareham RS. Carbohydrate recognition through non-covalent interactions: a challenge for biomimetic and supramolecular chemistry. Angew Chem Int Ed. 1999;38:2978–96.
3. Arnold MA, Small GW. Noninvasive glucose sensing. Anal Chem. 2005;77:5429–39.
4. Borisov SM, Wolfbeis OS. Optical biosensors. Chem Rev. 2008;108:423–61.
5. Kubik S. Synthetic lectins. Angew Chem Int Ed. 2009;48:1722–5.

6. Davis AP. Synthetic lectins. Org Biomol Chem. 2009;7:3629–38.
7. Mazik M. Molecular recognition of carbohydrates by acyclic receptors employing noncovalent interactions. Chem Soc Rev. 2009;38:935–56.
8. Kejík Z, Bříza T, Králová J, Martásek P, Král V. Selective recognition of a saccharide-type tumor marker with natural and synthetic ligands: a new trend in cancer diagnosis. Anal Bioanal Chem. 2010;398:1865–70.
9. Asensio JL, Ardá A, Cañada FJ, Jiménez-Barbero J. Carbohydrate-aromatic interactions. Acc Chem Res. 2013;46:946–54.
10. Wu X, Li Z, Chen XX, Fossey JS, James TD, Jiang YB. Selective sensing of saccharides using simple boronic acids and their aggregates. Chem Soc Rev. 2013;42:8032–48.
11. Miron CE, Petitjean A. Sugar recognition: designing artificial receptors for applications in biological diagnostics and imaging. ChemBioChem. 2015;16:365–79.
12. Fukuhara G. Analytical supramolecular chemistry: colorimetric and fluorimetric chemosensors. J Photochem Photobiol C Photochem Rev. 2020;42:100340.
13. Hu W, Zhang G, Zhou Y, Xia J, Zhang P, Xiao W, et al. Recent development of analytical methods for disease-specific protein *O*-GlcNAcylation. RSC Adv. 2023;13:264–80.
14. Cao X, Yao J, Jia M, Shen X, Zhang J, Ju S. Serum CCAT2 as a biomarker for adjuvant diagnosis and prognostic prediction of cervical cancer. J Ovar Res. 2022;15:20.
15. Matsunaga T, Saito H, Kuroda H, Osaki T, Takahashi S, Iwamoto A, et al. CA19-9 in combination with P-CRP as a predictive marker of immune-related adverse events in patients with recurrent or unresectable advanced gastric cancer treated with nivolumab. BMC Cancer. 2022;22:418.
16. Cen P, Ni X, Yang J, Graham DY, Li M. Circulating tumor cells in the diagnosis and management of pancreatic cancer. Biochimica et Biophysica Acta. 2012;1826:350–6.
17. James TD, Sandanayake KRAS, Shinaki S. Chiral discrimination of monosaccharides using a fluorescenct molecular sensor. Nature. 1995;374:345–7.
18. Yashima E, Nimura T, Matsushima T, Okamoto Y. Poly((4-dihydroxyborophenyl)acetylene) as a novel probe for chirality and structural assignments of various kinds of molecules including carbohydrates and steroids by circular dichroism. J Am Chem Soc. 1996;118:9800–1.
19. Samoei GK, Wang W, Escobedo JO, Xu X, Schneider HJ, Cook RL, et al. A chemomechanical polymer that functions in blood plasma with high glucose selectivity. Angew Chem Int Ed. 2006;45:5319–22.
20. Yang X, Lee MC, Sartain F, Pan X, Lowe CR. Designed boronate ligands for glucose-selective holographic sensors. Chem Eur J. 2006;12:8491–7.
21. Wang L, Li Y. Luminescent nanocrystals for nonenzymatic glucose concentration determination. Chem Eur J. 2007;13:4203–7.
22. Schiller A, Wessling RA, Singaram B. A fluorescent sensor array for saccharides based on boronic acid appended bipyridinium salts. Angew Chem Int Ed. 2007;46:6457–9.
23. Edwards NY, Sager TW, McDevitt JT, Anslyn EV. Boronic acid based peptidic receptors for pattern-based saccharide sensing in neutral aqueous media, an application in real-life samples. J Am Chem Soc. 2007;129:13575–83.
24. Pal A, Bérubé M, Hall DG. Design, synthesis, and screening of a library of peptidyl bis(boroxoles) as oligosaccharide receptors in water: identification of a receptor for the tumor marker TF-antigen disaccharide. Angew Chem Int Ed. 2010;49:1492–5.
25. Carrod AJ, Graglia F, Male L, Duff CL, Simpson P, Elsherif M, et al. Photo- and electrochemical dual-responsive iridium probe for saccharide detection. Chem Eur J. 2022;28:e202103541.
26. Kobayashi K, Asakawa Y, Kato Y, Aoyama Y. Complexation of hydrophobic sugars and nucleosides in water with tetrasulfonate derivatives of resorcinol cyclic tetramer having a polyhydroxy aromatic cavity: importance of guest-host CH-π interaction. J Am Chem Soc. 1992;114:10307–13.
27. Chinnayelka S, McShane MJ. Microcapsule biosensors using competitive binding resonance energy transfer assays based on apoenzymes. Anal Chem. 2005;77:5501–11.
28. Schmuck C, Schwegmann M. Recognition of anionic carbohydrates by an artificial receptor in water. Org Lett. 2005;7:3517–20.
29. Mazik M, Cavga H. Carboxylate-based receptors for the recognition of carbohydrates in organic and aqueous media. J Org Chem. 2006;71:2957–63.
30. Waki M, Abe H, Inouye M. Translation of mutarotation into induced circular dichroism signals through helix inversion of host polymers. Angew Chem Int Ed. 2007;46:3059–61.
31. Goto H, Furusho Y, Yashima E. Double helical oligoresorcinols specifically recognize oligosaccharides via heteroduplex formation through noncovalent interactions in water. J Am Chem Soc. 2007;129:9168–74.
32. Reenberg T, Nyberg N, Duus JØ, van Dongen JLJ, Meldal M. Specific recognition of disaccharides in water by an artificial bicyclic carbohydrate receptor. Eur J Org Chem. 2007;5003-9.
33. Ferrand Y, Crump MP, Davis AP. A synthetic lectin analog for biomimetic disaccharide recognition. Science. 2007;318:619–22.
34. Striegler S, Gichinga MG. Disaccharide recognition by binuclear copper(II) complexes. Chem Commun. 2008;5930-2.
35. Barwell NP, Crump MP, Davis AP. A synthetic lectin for β-glucosyl. Angew Chem Int Ed. 2009;48:7673–6.
36. Ke C, Destecroix H, Crump MP, Davis AP. A simple and accessible synthetic lectin for glucose recognition and sensing. Nat Chem. 2012;4:718–23.
37. Rauschenberg M, Bandaru S, Waller MP, Ravoo BJ. Peptide-based carbohydrate receptors. Chem Eur J. 2014;20:2770–82.
38. Mooibroek TJ, Casas-Solvas JM, Harniman RL, Renney CM, Carter TS, Crump MP, et al. A threading receptor for polysaccharides. Nat Chem. 2016;8:69–74.
39. Behren S, Yu J, Pett C, Schorlemer M, Heine V, Fischöder T, et al. Fucose binding motifs on mucin core glycopeptides impact bacterial lectin recognition. Angew Chem Int Ed. 2023;62:e202302437.
40. Fukuhara G, Inoue Y. Oligosaccharide sensing with chromophore-modified curdlan in aqueous media. Chem Commun. 2010;46:9128–30.
41. Ogawa K, Miyagi M, Fukumoto T, Watanabe T. Effect of 2-chloroethanol, dioxane, or water on the conformation of a gel-forming β-1,3-D-glucan in DMSO. Chem Lett. 1973;2:943–6.
42. Deslandes Y, Marchessault RH, Sarko A. Triple-helical structure of (1→3)-*β*-D-glucan. Macromolecules. 1980;13:1466–71.
43. Numata M, Shinkai S. 'Supramolecular wrapping chemistry' by helix-forming polysaccharides: a powerful strategy for generating diverse polymeric nano-architectures. Chem Commun. 2011;47:1961–75.
44. Eleftheriadou I, Grigoropoulou P, Katsilambros N, Tentolouris N. The effects of medications used for the management of diabetes and obesity on postprandial lipid metabolism. Curr Diabetes Rev. 2008;4:340–56.
45. Fukuhara G, Sasaki M, Numata M, Mori T, Inoue Y. Oligosaccharide sensing in aqueous media by porphyrin-curdlan conjugates: a prêt-á-porter rather than haute-couture approach. Chem Eur J. 2017;23:11272–8.
46. Sasaki M, Ryoson Y, Numata M, Fukuhara G. Oligosaccharide sensing in aqueous media using porphyrin-curdlan conjugates: an allosteric signal-amplification system. J Org Chem. 2019;84:6017–27.

47. Kurohara H, Hori Y, Numata M, Fukuhara G. Oligosaccharide sensing using fluorophore-probed curdlans in aqueous media. ACS Appl Polym Mater. 2023;5:2254–63.
48. Tamano K, Nakasha K, Iwamoto M, Numata M, Suzuki T, Uyama H, et al. Chiroptical properties of reporter-modified or reporter-complexed highly 1,6-glucose-branched β-1,3-glucan. Polym J. 2019;51:1063–71.
49. Mei J, Leung NLC, Kwok RTK, Lam JWY, Tang BZ. Aggregation-induced emission: together we shine, united we soar! Chem Rev. 2015;115:11718–940.
50. Felorzabihi N, Froimowicz P, Haley JC, Bardajee GR, Li B, Bovero E, et al. Determination of the Förster distance in polymer films by fluorescence decay for donor dyes with a nonexponential decay profile. J Phys Chem B. 2009;113:2262–72.
51. Sangghaleh F, Sychugov I, Yang Z, Veinot JGC, Linnros J. Near-unity internal quantum efficiency of luminescent silicon nanocrystals with ligand passivation. ACS Nano. 2015;9:7097–104.